THE ASTROPHYSICAL JOURNAL, 484:L71–L74, 1997 July 20

COMPLEMENTARY TRACE ELEMENT ABUNDANCES IN METEORITIC SiC GRAINS AND CARBON STAR ATMOSPHERES

KATHARINA LODDERS AND BRUCE FEGLEY, JR.
Planetary Chemistry Laboratory, Department of Earth and Planetary Sciences, Campus Box 1169, Washington University, St. Louis MO 63130-4899; lodders@levee.wustl.edu, bfegley@levee.wustl.edu
Received 1997 January 9; accepted 1997 May 1

ABSTRACT

Equilibrium condensation calculations successfully explain the complementary trace element abundance patterns observed in carbon star atmospheres and circumstellar SiC grains found in meteorites. Fractional trace element condensation into SiC depletes the gas in refractory trace elements, while more volatile elements remain in the gas. The observed complementary patterns imply that dust forms relatively close to the star, possibly during the minimum light phase in stellar variability cycles. Once the gas falls back onto the star during stellar contraction, photospheric abundances become relatively enriched in more volatile elements. The complementary trace element abundances link circumstellar SiC grains from meteorites to carbon star atmospheres.

Subject headings: stars: abundances — stars: carbon — stars: circumstellar matter — stars: variables: other

1. INTRODUCTION

Cool carbon stars with dusty circumstellar envelopes (CSEs) inject carbonaceous dust into the interstellar medium (ISM). Dust from C stars is 10–50% of the 0.35 $M_\odot$ of dust contributed to the ISM per year (Thronson et al. 1987). Low-resolution spectra (LRSs) of C stars commonly display the 11.3 μm SiC emission band, which is not surprising since SiC is a major condensate formed at C/O $\geq$ 1. Isotopic analyses of presolar graphite and SiC grains from meteorites indicate that these grains can originate in C star CSEs (Gallino et al. 1990; see review by Anders & Zinner 1993). Thus, grains from carbon stars were apparently present in the solar nebula.

Equilibrium condensation calculations (Lodders & Fegley 1995) show that the observed abundances of trace elements such as Ti, V, and *s*-process elements (e.g., Zr, Ba, Sr, rare earth elements [REEs]) in SiC (Amari et al. 1995) are consistent with fractional condensation into SiC grains in CSEs. These calculations imply that the SiC grains and the residual gas display complementary abundance patterns. Here we show that observed abundance patterns in C star atmospheres are indeed complementary to those observed in SiC grains, providing another link between meteoritic SiC grains and C stars.

2. THERMODYNAMIC MODELS OF SiC GRAIN CONDENSATION

We previously modeled thermochemical equilibrium chemistry of major and trace elements in C stars (Lodders & Fegley 1993, 1995; hereafter LF93, LF95). The major element condensation sequence (TiC, graphite, and SiC) is sensitive to the total pressure (P) and the C/O ratio. Condensation temperatures for a wide P-C/O range are listed in LF95. Lambert et al. (1986) determined that typical C star-C/O ratios are 1–1.2. For carbon stars with $T_{\rm eff}$ = 2500–2800 K, model atmospheres by Jorgensen, Johnson, & Nordlund (1992) indicate pressures of $\sim 10^{-5}$ to 10^{-9} bars (10–10^{-3} dyne cm^{-2}) for temperatures between $\sim$1500 and 2300 K. In these P and T ranges, the condensation sequence TiC, graphite, and SiC occurs (LF93, LF95), in agreement with observations of TiC crystals in circumstellar graphite spheres and the absence of SiC grains in these graphites (Bernatowicz et al. 1996).

Less abundant elements such as Zr, V, Nb, Mo, Sr, Ba, and the REE generally condense in solid solution with preexisting phases such as TiC or SiC. Either carbides (ZrC, HfC, $VC_{0.88}$, MoC), sulfides (SrS, BaS, LaS), or nitrides (AlN) can form solid solutions with TiC and SiC (LF93, LF95). Incorporation of these elements into TiC or SiC depends on their volatility. Very refractory carbides such as ZrC or MoC readily form solid solutions with TiC, and TiC-ZrC-MoC solid solution grains were observed by Bernatowicz et al. (1996) in presolar graphite grains. Such refractory carbides can completely dissolve into SiC once it forms. The REE are less refractory and do not fully condense into TiC at high temperatures but are completely scavenged into SiC at lower temperatures. Barium and Sr are more volatile and require the lowest temperatures to fully condense into SiC.

Ion microprobe analyses of circumstellar SiC grains revealed about nine types of CI-chondrite normalized abundance patterns (Amari et al. 1995), of which three are shown in Figure 1*a*–1*c*. The individual patterns shown in a given plot are similar, but absolute abundances in individual grains may differ by up to a factor of 10 for most elements. This spread in abundances is probably larger than the analytical uncertainties. Instead of modeling an individual pattern from a single grain, we use the average abundances for each type of pattern in Figure 1*a*–1*c*.

To model these patterns, we used a gas of solar composition (Anders & Grevesse 1989) with an increased carbon abundance (C/O = 1.05) and a total pressure of $P = 10^{-5}$ bars. Under these conditions, the condensation temperatures of TiC, graphite, and SiC are 1702, 1600, and 1544 K, respectively, consistent with the observations of TiC in graphite (Bernatowicz et al. 1996). This condensation sequence occurs in a P range of 3×10^{-7} to 3.4×10^{-5} bars for C/O = 1.05 (LF95). We model trace element condensation using $P = 10^{-5}$ bars to illustrate how the patterns can be established. Lower total pressures uniformly decrease the condensation temperatures for all elements without altering relative abundance patterns.

Thermodynamic modeling of the abundance patterns required enriched *s*-process element abundances, consistent with observed *s*-process enrichments in *N*-type carbon stars

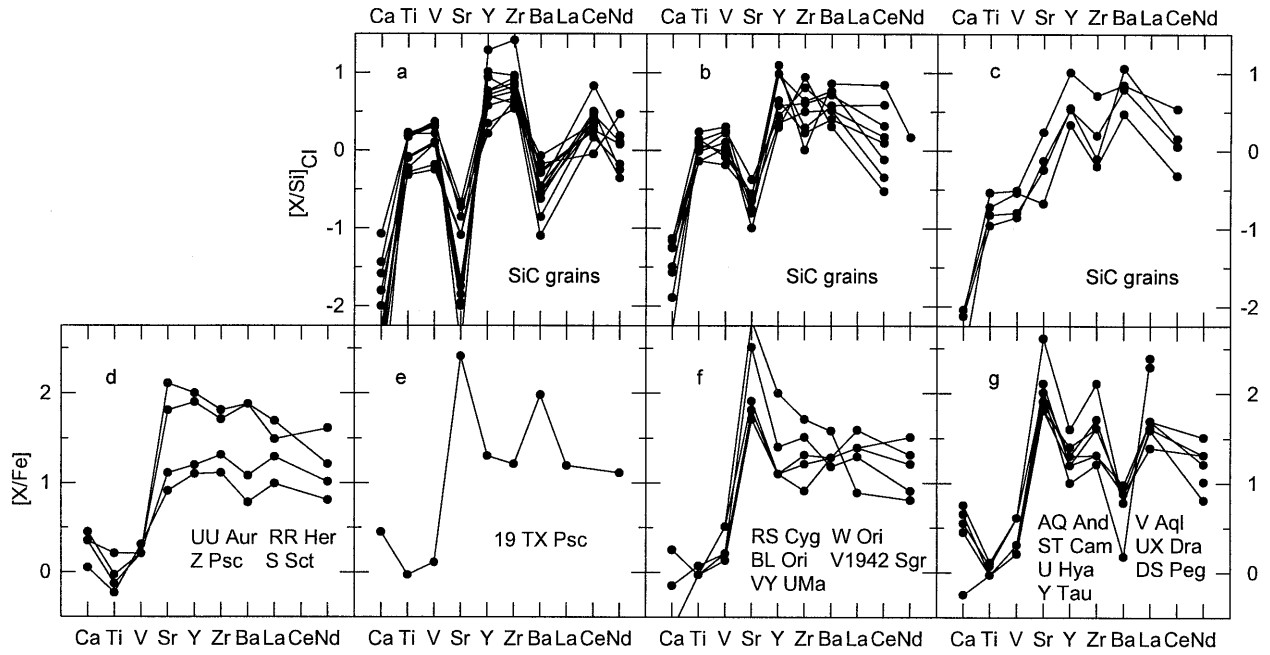

FIG. 1.—Top panel shows three types of CI-chondrite and Si normalized trace element abundance patterns in circumstellar SiC grains from the Murchison meteorite (Amari et al. 1995). The notation is $[X/Si]_{CI} = \log (X/Si)_{grain} - \log (X/Si)_{CI\text{-}chondrites}$. The bottom panel gives solar and Fe-normalized abundance patterns from N-type carbon stars from Utsumi (1985) renormalized to the solar abundances by Anders & Grevesse (1989). The SiC grain and the stellar patterns are arranged to show their complementary nature.

(Kilston 1975; Utsumi 1985). We used a uniform enrichment for *s*-process elements in the calculations because abundance variations caused by *s*-processing of different nuclides for the elements of interest lead to similar abundance increases. Only about half of all Si condenses as SiC. Thus, elements present at solar abundance in SiC plot at log 2 = 0.3 in Figures 1*a*–1*c*, and *s*-process elements that are enriched and completely condensed into SiC plot above 0.3. In the following, we always refer to the Si-normalized abundances when discussing trace element abundances in SiC.

3. EXAMPLES OF THERMODYNAMIC MODELING OF TRACE ELEMENT PATTERNS IN SiC GRAINS

The patterns in Figure 1*a* are characterized by strong depletions of the most volatile elements Sr and Ba (the Ca depletion is discussed below). The Ti and V abundances plot around one times CI-chondritic (= solar). Yttrium, Zr, and the REE are enriched by about a factor of up to 10. The enrichment factor of *s*-process elements is found by comparing the Ti and Zr abundances. Both elements are highly refractory and condense closely together. Thus, the Zr/Ti ratio indicates the enrichment of *s*-process elements, which is about 3–4 times solar for the grains in Figure 1*a*. Titanium, V, Y, Zr, and REE condense into SiC as soon as it forms. Trace element condensation into SiC continues until grains are removed from equilibrium with the gas. The depletion of the two most volatile elements, Sr and Ba, indicates that gas-solid equilibrium stopped at ~1300 K.

Some grains in Figure 1*a* have relative Ti and V abundances of ~2, which indicates that the full complement of Ti and V was incorporated into SiC, while Ti and V abundances of some other grains are as low as 0.5, an indication of uniform loss of V and Ti. Some removal of very refractory Ti-Zr-carbides may have occurred prior to SiC formation (see below).

The trace element patterns in Figure 1*b* are also produced by fractional condensation from a gas containing *s*-process elements at 3–4 times solar abundances. Barium is as abundant as Y, Zr, and the REE, while Sr is depleted. Although Sr and Ba have similar volatility when compared to the other more refractory trace elements, Sr is somewhat more volatile than Ba. The SiC grains in Figure 1*b* equilibrated with the gas to temperatures between 1300 and 1250 K. At 1250 K, Ba and Sr would be almost fully condensed, which is not observed, and thus 1250 K is a lower temperature limit. These element patterns also require removal of some of the very refractory elements Ti, V, and Zr prior to SiC formation. TiC condenses about 160 K higher than SiC, and carbides such as ZrC or $VC_{0.88}$ dissolve in TiC. Early-forming carbide grains may have been expelled from the SiC grain-forming region so that only a few ultrarefractory grains were trapped in SiC. Such ultrarefractory TiC grains seem to have served as nucleation seeds in circumstellar graphite grains (Bernatowicz et al. 1996), and a similar situation may apply for the SiC grains.

Figure 1*c* shows SiC grains with more complex abundance patterns that are also consistent with fractional condensation. These patterns display a Sr depletion and a Ba enrichment, which is unexpected as Ba and Sr have similar volatilities. For these patterns, we need *s*-process element abundances of 10 times solar and removal of about 90% of all Ti, V, Zr, Y, and REE prior to SiC formation. In addition to highly refractory Zr and V, this TiC may have also incorporated some of the REE. Alternatively, the first SiC grains to condense may have scavenged highly refractory elements and REE before being removed from further equilibrium with the gas, leaving Sr and Ba behind. Subsequently, other SiC grains formed, incorporated the refractory elements left in the gas, and partially incorporated Ba and Sr to establish the patterns seen in Figure 1*c*.

Amari et al. (1995) measured low abundances of Ca, Al, and Fe (not plotted) in all SiC grains. The observed abundances, in particular those for Fe, are lower than predicted by ideal solubility. In contrast to trace elements, Ca, Al, and Fe may form their own condensates instead of dissolving into SiC. The condensation temperatures of Fe (as Fe_3C or Fe-metal at 1275 K), AlN (1242 K), and CaS (1220 K) are close to the temperatures at which larger amounts of CaS, AlN, and Fe are expected to dissolve into SiC. The formation of Fe, Fe_3C, CaS, and AlN may compete with solid solution formation in SiC.

Although observed Fe and Ca abundances in N stars seem to be close to solar (Lambert et al. 1986), the assumption of solar Ca, Al, and Fe abundances may not be valid. The carbon stars in which the presolar SiC grains originated more than 4.6 Gyr ago may have had subsolar metallicities. Yet another possibility is that at least some grains originated from CH stars, which have subsolar metallicities. Although CH stars are very rare, LF95 suggest that they could be possible sources for some of the presolar SiC grains. Nevertheless, the low Fe abundance in SiC grains merits further investigation.

4. TRACE ELEMENT PATTERNS IN N STAR ATMOSPHERES

The preceding discussion indicates that the observed trace element patterns in circumstellar SiC grains can be explained by fractional condensation. Removal of trace elements from the gas into SiC is governed by volatility: refractory elements enriched in the SiC grains are depleted in the residual gas, while volatile elements depleted in the SiC grains are enriched in the residual gas. We now show that the (limited) abundance data for C stars have the predicted complementary patterns.

Spectra from cool carbon stars are difficult to analyze because of line blending, and only a few analyses of heavy elements are available. We use data from Utsumi (1985), who made most of the observations of heavy element abundances in C stars. Close inspection of Utsumi's data shows that abundances (normalized to solar and Fe) in the cooler N-type C stars display several patterns. In Figure 1*d*–1*g* we plot four types of patterns that are found in 17 of the 21 N-type C stars in Utsumi's sample of thirty N-, R-, and J-type C stars.

Figure 1*d* shows patterns generally assumed to be characteristic for N stars with about solar abundances for Ca, Ti, V, and *s*-process elements at about 10–100 times solar. Figures 1*e*–1*g* display other patterns, generally with *s*-process enrichments but also showing Sr (and Ba) enrichments (Figs. 1*e* and 1*f*), and more complex patterns with Sr, Zr enrichments and Ba depletions (Fig. 1*g*). The SiC grain and stellar trace element patterns in Figure 1 are arranged to show the complementary nature of the pairs shown as Figures 1*a* and 1*e*, 1*b* and 1*f*, and 1*c* and 1*g*.

The stellar abundance patterns are complementary to those in SiC because fractional condensation into SiC grains enriches the gas in volatile elements (i.e., Sr, Ba). We do not believe that the different stellar abundance patterns are analytical artifacts. Utsumi (1985) carefully selected bands which were free of blending and applied the same curve-of-growth method to all stars in his sample. Utsumi gives an uncertainty of ~0.4 dex in the solar-normalized abundances, except for the REE, where his uncertainties may be larger. The stated error bars easily fall within the wide abundance range spanned by the individual patterns, and, as with patterns in SiC grains, we look at the overall structure of the patterns. Although absolute abundances may vary, it is unlikely that the uncertainties would change the relative abundance patterns dramatically. Systematic errors in Utsumi's analyses are also unlikely to generate different abundance patterns.

Kilston (1975) reported elemental abundances for eight N stars. Similar abundances result for stars common to both Kilston's and Utsumi's observations when both data sets are normalized to the same solar abundances. Unfortunately, Kilston did not determine Sr abundances, which are critical for determining the type of abundance patterns.

5. STELLAR ABUNDANCE PATTERNS AND OTHER PHYSICAL PARAMETERS IN N STARS

If we accept that the stellar abundance patterns are real, other stellar properties may relate the stars in the abundance pattern groups in Figures 1*d*–1*g*. However, we found no apparent relationships between elemental abundance patterns and spectral type, variable type or period (the stars are mainly SR and Lb variables), photospheric radius, location of the inner dust shell radius, mass-loss rate, expansion velocity, $^{12}C/^{13}C$ ratio or the C/O ratio (Bergeat, Sibille, & Lunel 1978; Lambert et al. 1986; Olofsson et al. 1993a, 1993b). Most stars have the SiC 11.3 μm band (LRS = 4n; Neugebauer et al. 1986) showing that SiC is a potential sink for trace elements. All stars in Figure 1*g* have LRS = 4n, while some stars from Figures 1*d*–1*f* (S Sct, TX Psc, RS Cyg, BL Ori, V1942 Sgr) have LRS = 1n, indicating the absence of SiC dust emission. Three of the five stars in Figure 1*f* have LRS = 1n, but more analytical data are needed to tell if this is statistically significant.

Technetium spectral lines may be common to all stars showing fractionated patterns in Figures 1*e*–1*g* (Little, Little-Marenin, & Bauer 1987). Stars with unfractionated (Fig. 1*d*) and unique abundance patterns may not contain Tc. Technetium was not detected in UU Aur (Fig. 1*d*) or in two (X Cnc, SS Vir) of the four ungrouped stars with abundance patterns for which no complementary patterns are found yet in SiC. The presence or absence of Tc should be checked for all stars to see if Tc is a tracer for the groupings in Figure 1.

Stars with an unfractionated pattern (Fig. 1*d*) may be binaries or objects with detached CSE. The absence of Tc in RR Her, Z Psc, and S Sct may be a sensitive test for binarity (see Alksne, Alksnis, & Dzervitis 1991). In a binary system, overflowing, accreting matter could determine the abundance pattern. On the other hand, the detached CSE of S Sct (LRS = 1n) is well established (see Olofsson et al. 1993a, 1993b) and it plots into the VIa region of the *IRAS* color diagram. This region indicates far distant fossil dust shells (van der Veen & Habing 1988; Loup et al. 1993). Atmospheric trace element abundances cannot be altered by fractional condensation into SiC if no dust formation is currently taking place.

Other stars with LRS = 1n (TX Psc, V1942 Sgr) also have 60 μm excesses and plot into field VIa of the *IRAS* color diagram. The fractionated abundance patterns and absence of the 11.3 μm SiC emission may indicate that dust formation has stopped relatively recently and that atmospheric compositions were not yet altered by mixing with fresh, unfractionated material from stellar interiors. VY UMa also plots into region VIa of the *IRAS* color diagram but has SiC in emission showing ongoing dust formation and the presence of an old dust shell.

However, we find no way to group stars showing fraction-

ated patterns (Figs. 1*e*–1*g*) other than by their common trace element patterns. We suggest that stellar variability is the key to understanding which abundance patterns are observed.

6. POSSIBLE PHYSICAL SETTINGS FOR FRACTIONAL CONDENSATION IN CSE

Periodic changes in luminosities, effective temperatures, and photospheric radii alter stellar atmospheric structure. Bergeat & Sibai (1983) examined the pulsation of carbon Miras and derived photospheric radii and temperatures as a function of the light curve phase. At maximum light, effective temperatures are at their maximum and photospheric radii (R_{ph}) at their minimum values. For the carbon Mira variable U Cyg, the effective temperature is ~2300 K and $R_{ph} \sim 40\ R_{\odot}$ at maximum light. At minimum light, the effective temperature drops to ~1800 K and R_{ph} increases to 360 $R_{\odot}$ (Figs. 4 and 5 in Bergeat & Sibai 1983). Such periodic changes in temperature and radii must affect the dust-forming region. LeBertre (1988) notes that the equilibrium temperature at a given distance from the central star changes with phase and that grains condense between maximum and minimum, while between minimum and maximum, grains evaporate.

We now follow a pulsation cycle and examine fractional condensation of trace elements into SiC. Most shell models have been applied to Mira variables (Bergeat & Sibai 1983; LeBertre 1988), while the stars here are SR and Lb variables. However, we assume that similar mechanisms apply. Several models of mass-loss mechanisms exist (see Danchi & Bester 1995), and we adopt a model involving thermal pulses and stellar winds driven by radiation pressure on dust grains. At maximum light, the star has its smallest radius and highest effective temperature. Periodic pulses lead to shock waves, and energy dissipation causes extension of the photospheric radius and decrease in temperature. The star moves into its minimum light phase where the photospheric radius increases and effective temperature decreases. If temperatures in the surrounding stellar atmosphere become low enough, grain condensation takes place at a temperature T_{grain} and radius R_{grain}. The inner edge of the dust-forming region in the CSE is $R_{grain}/R_{ph} \geq 1.5$–4 (Bergeat et al. 1976; Danchi & Bester 1995). In the dust-forming region, the gas becomes depleted in refractory elements owing to their removal into SiC, while volatile Ba and Sr stay behind in the gas.

Several models show that radiation pressure on dust is responsible for initiating the mass-loss process (see, e.g., Gail & Sedlmayr 1987; Fleischer, Gauger, & Sedlmayr 1992; Höfner, Feuchtinger, & Dorfi 1995). Once grains form, radiation pressure accelerates them, and they move to outer regions of the CSE. Dust-gas momentum coupling can create strong stellar winds, and the mass-loss rate depends on the amount of dust present. The SR and Lb variables generally have smaller amounts of dust in their CSE and smaller mass-loss rates when compared to Mira variables. Work by Bowen (1988) suggests that shock waves generated by pulsation are also necessary to increase mass-loss rates in long-period variables. Smaller amounts of dust and more irregular pulsation properties of the Lb and SR variables may not create the mass-loss rates necessary to allow effective dust-gas coupling. If so, dust grains may be lost while Ba- and Sr-enriched gas stays behind in the grain-forming region.

Once the star moves back to maximum light, it contracts, which leads to a gravity-driven fallback of the gas onto the photosphere (and thus the line-forming region). The gas at the photosphere becomes enriched in Ba and Sr from the infalling gas. It may take several pulsation cycles for the Sr and Ba enrichment to become spectroscopically detectable.

This scenario may be similar to that proposed to explain metal-poor post-asymptotic giant branch (AGB) stars. These have either accreted dust-depleted matter from a binary companion or lost dust when a drop in AGB mass loss led to a lack of dynamical support and caused volatile, rich gas fallback onto the star (Mathis & Lamers 1992; Waters, Trams, & Waelkens 1992).

It is desirable to test the model here with more analyses of elemental abundances for carbon stars. In particular it would be interesting to check for abundance variations as a function of light curve, variability type, LRS classification, and *IRAS* far-infrared properties.

We thank U. G. Jorgensen for a detailed and helpful referee report. This work was supported by NASA grant NAGW 3070.

REFERENCES

Alksne, Z. K., Alksnis, A. K., & Dzervitis, U. K. 1991, Properties of Galactic Carbon Stars (Malabar, FL.: Orbit Book Co.)
Amari, S., Hoppe, P., Zinner, E., & Lewis, R. S. 1995, Meteoritics, 30, 679
Anders, E., & Grevesse, N. 1989, Geochim. Cosmochim. Acta, 53, 197
Anders, E., & Zinner, E. 1993, Meteoritics, 28, 490
Bergeat, J., Lefevre, J., Kandel, R., Lunel, M., & Sibille, F. 1976, A&A, 52, 245
Bergeat, J., & Sibai, A. M. 1983, A&A, 119, 207
Bergeat, J., Sibille, F., & Lunel, M. 1978, A&A, 64, 423
Bernatowicz, T. J., Cowsik, R., Gibbons, P. C., Lodders, K., Fegley, B., Amari, S., & Lewis, R. S. 1996, ApJ, 472, 760
Lewis, R. S. 1996, ApJ, 472, 760
Bowen, G. H. 1988, ApJ, 329, 299
Danchi, W. C., & Bester, M. 1995, Ap&SS, 224, 339
Fleischer, A. J., Gauger, A., & Sedlmayr, E. 1992, A&A, 266, 321
Gail, H. P., & Sedlmayr, E. 1987, A&A, 171, 197
Gallino, R., Busso, M., Picchio, G., & Raiteri, C. M. 1990, Nature, 348, 298
Höfner, S., Feuchtinger, M. U., & Dorfi, E. A. 1995, A&A, 297, 815
Jorgensen, U. G., Johnson, H. R., & Nordlund, A. 1992, A&A, 261, 263
Kilston, S. 1975, PASP, 87, 189
Lambert, D. L., Gustafsson, B., Eriksson, K., & Kinkle, K. H. 1986, ApJS, 62, 373
LeBertre, T. 1988, A&A, 190, 179
Little, S. J., Little-Marenin, I. R., & Bauer, W. H. 1987, ApJ, 94, 981
Lodders, K., & Fegley, B. 1993, Meteoritics, 27, 250 (LF93)
———. 1995, Meteoritics, 30, 661 (LF95)
Loup, C., Forveille, T., Omont, A., & Paul, J. F. 1993, A&AS, 99, 291
Mathis, J. S., & Lamers, H. J. G. L. M. 1992, A&A, 259, L39
Neugebauer, G., et al. 1986, A&AS, 65, 607
Olofsson, H., Eriksson, K., Gustafsson, B., & Carlström, U. 1993a, ApJS, 87, 267
———. 1993b, ApJS, 87, 305
Thronson, H. A., Latter, W. B., Black, J. H., Bally, J., & Hacking, P. 1987, ApJ, 322, 770
Utsumi, K. 1985, Proc. Japan Acad. B61, 193
van der Veen, W. E. C. J., & Habing, H. J. 1988, A&A, 194, 125
Waters, L. B. F. M., Trams, N. R., & Waelkens, C. 1992, A&A, 262, L37